Journal of Electrical Engineering, Vol. 76, No. 6, 2025, pp. 485-498
https://reference-global.com/journal/JEE

Fluorine-doped SnO_2 thin films for solar cells: Development and comparative analysis of spray pyrolysis and spin coating techniques

Sherif A. Khaleel[1,*], Ahmed M. Abdelsamad[2,3], Gaber Magdy[4,5], Mohamed I. Shehata[1], Nehad A. Zidan[3]

In this study, fluorine-doped tin oxide (FTO) thin films were synthesized using two low-cost solution-based techniques, homemade spray pyrolysis and spin coating, conducted at a substrate temperature of 500 °C. Fluorine was introduced as an n-type dopant in concentrations ranging from 10 to 40 wt% to enhance the electrical conductivity and optical transmittance of the films. The structural, morphological, and optoelectronic properties of the films were characterized via XRD, SEM, UV-Vis spectroscopy, and Hall effect analysis. The spray-deposited FTO films exhibited superior performance, with optimized samples (at 30 wt% F) achieving a sheet resistance of 20 Ω/□, optical transmittance of 80%, and a figure of merit (FOM) of 5.37×10^{-3} Ω^{-1}. In contrast, spin-coated films showed higher resistivity, lower mobility, and reduced FOM (e.g., 1.53×10^{-3} Ω^{-1} at 840 nm thickness), attributed to inferior film densification and increased structural defects. The results demonstrate that spray pyrolysis enables the formation of dense, well-crystallized FTO layers with enhanced carrier transport and transparency, making it a more suitable deposition technique for optoelectronic and photovoltaic applications.

Keywords: fluorine tin oxide, spray technique, spin coating, optical transmission, XRD, sheet resistance

1 Introduction

Transparent conducting oxide (TCO) thin films are essential components in contemporary optoelectronic and photovoltaic applications, owing to their rare combination of high optical transparency and electrical conductivity. These materials are widely employed in solar cells, light-emitting diodes (LEDs), flat-panel displays, touchscreens, smart windows and IoT application for G communications systems [1-3] .where they function as transparent electrodes that facilitate efficient charge transport while allowing maximum light transmission [4, 5]. Among these applications, solar energy harvesting has gained significant attention as a sustainable and renewable energy solution. In photovoltaic devices, TCOs serve as front contacts in solar cells, ensuring minimal optical loss and effective charge collection, which directly impacts the overall device efficiency. Therefore, developing a stable, low-cost TCO remains a key challenge that must be addressed [6, 7].

Among various TCO materials, fluorine-doped tin oxide (FTO) stands out as a promising candidate owing to its excellent thermal stability, chemical resistance, and low-cost fabrication compared to widely used alternatives like indium tin oxide (ITO) and aluminum-doped zinc oxide (AZO) [8-10]. Unlike ITO, which suffers from the scarcity and high cost of indium, FTO is composed of abundant and inexpensive raw materials, making it a more economically viable choice for large-scale production [11]. Furthermore, FTO films exhibit remarkable mechanical durability, which makes them well-suited for high-temperature environments and various photovoltaic applications, including thin-film, perovskite, and dye-sensitized solar cells (DSSCs) [12, 13].

The performance of FTO thin films is highly dependent on the deposition technique, which influences their structural, electrical, and optical properties. Several fabrication methods have been explored, including chemical vapor deposition (CVD) [14], pulsed laser deposition (PLD) [15], sol-gel processing [16], and magnetron sputtering [17]. However, spray pyrolysis has attracted considerable interest as a cost-effective and scalable deposition method capable of producing high-quality FTO films with controlled doping levels.

[1] Department of Electronics & Communications Engineering, College of Engineering and Technology, Arab Academy for Science, Technology and Maritime Transport (AASTMT), Aswan 81511, Egypt
[2] Department of Basic and Applied Science, College of Engineering and Technology, Arab Academy for Science, Technology and Maritime Transport (AASTMT), Aswan 81511, Egypt
[3] Engineering Physics and Mathematics Department, Faculty of Engineering – Mataria, Helwan University, Cairo, Egypt
[4] Department of Electrical Engineering, Faculty of Energy Engineering, Aswan University, Aswan 81528, Egypt
[5] Faculty of Engineering, King Salman International University, El-Tor, South Sinai 46511, Egypt
sherif.abdalla@aast.edu

https://doi.org/10.2478/jee-2025-0051, Print (till 2015) ISSN 1335-3632, On-line ISSN 1339-309X

This technique involves atomizing a precursor solution onto a heated substrate, where it undergoes pyrolytic decom-position to form a uniform film. The process parameters, including precursor concentration, spray rate, and substrate temperature, significantly influence the crystallinity, electrical conductivity, and optical transparency of the resulting FTO thin films.

Spin coating is another widely used deposition technique for fabricating TCO thin films, valued for its low cost, simplicity, and capability to yield uniform and smooth coatings [18]. This technique involves depositing a liquid precursor solution onto a rotating substrate, where centrifugal forces spread the solution into a thin, uniform layer before it undergoes thermal annealing to achieve the desired film properties. The thickness and uniformity of spin-coated films are primarily influenced by parameters such as spin speed, solution viscosity, and drying conditions. Compared to spray pyrolysis, spin coating offers precise thickness control and is commonly employed in laboratory-scale studies for developing TCO-based optoelectronic devices [19]. However, comparative studies analyzing the performance of FTO films produced via spray pyrolysis and spin coating remain limited.

In this study, FTO thin films were synthesized using two distinct deposition methods: homemade spray pyrolysis deposition (SPD) and spin coating deposition (SCD). Both techniques were carried out at a controlled substrate temperature of 500 °C to optimize the films' crystallinity and electrical performance. The deposited films were characterized using X-ray diffraction (XRD) for structural analysis, UV-Vis spectroscopy to evaluate optical transmittance measurements, and Hall effect analysis to determine electrical conductivity and carrier concentration. This comparative study aims to provide insights into the advantages and limitations of both fabrication techniques, with a particular focus on their applicability in solar cell technologies. By analyzing the structure-property relationships of FTO films, we seek to optimize their performance for efficient transparent electrodes in next-generation photovoltaic devices.

2 Experimental works

2.1 Thin film deposition by SPD

FTO thin films are fabricated via SPD on soda-lime glass (SLG) substrates, maintained at a substrate temperature of 500 °C. The precursor solution was formulated by dissolving stannous chloride dihydrate ($SnCl_2{\cdot}2H_2O$) in methanol, with glacial acetic acid added to promote ionization. Fluorine was introduced as an n-type dopant by adding 0.05 moles of hydrofluoric acid (HF), with doping concentrations varied at 10, 20, 30, and 40 wt% of F. The solution was stirred at 70 °C for 30 minutes to ensure complete dissolution and uniform mixing. The fluorine doping concentration range of 10-40 wt% was deliberately chosen because concentrations below 10 wt% generally do not provide sufficient carrier enhancement, while levels above 40 wt% often degrade crystallinity and reduce optical transparency due to increased scattering centres.

Before the deposition process, the SLG substrates were ultrasonically cleaned in methanol and deionized water for 15 minutes each, followed by drying at 100°C. The prepared precursor solution was atomized and sprayed onto the preheated substrates using a spray system, which generates a fine mist, resulting in improved film uniformity and homogeneity compared to conventional spray techniques. The deposition process was performed in a sequential layer-by-layer manner, incorporating a 5-minute interval between successive layers to optimize the film growth.

The deposition duration varied between 5 and 30 minutes, with an optimal deposition time of 15 minutes at a fixed substrate temperature of 500 °C. The spray parameters, including air pressure 600 kPa and nozzle-substrate distance 20 cm, were carefully controlled to achieve uniform film thickness as indicated in the spray mechanism in Fig. 1. After the deposition process, the films were left to cool naturally to ambient temperature on the heated substrate to ensure structural stability.

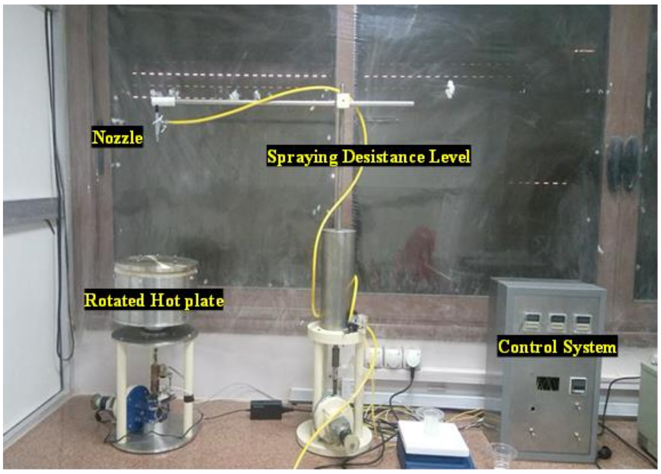

Fig. 1. Homemade spray deposition mechanism

2.2 Thin film deposition by SCD

The deposition mechanism of FTO layers using the SCD technique, as shown in Fig. 2, is illustrated in this section, starting with the materials preparation. The stannous chloride dihydrate ($SnCl_2{\cdot}2H_2O$) and the hydro-fluoric acid (HF) are used to form the precursor solution. Stannous chloride is dissolved in an appropriate solvent to form a uniform solution, after which hydrofluoric acid (HF) is incrementally added to achieve fluorine doping at specified concentrations of 10, 20, 30, and 40 wt% of F. The prepared solution was deposited onto a pre-cleaned substrate of SLG, which was then spun at high speeds of 3000 rpm to achieve uniform film thickness. The precursor solution was deposited on the substrate with a height of 2 cm, with a 1 drop for 80 seconds maintained on a hot plate at 200 °C for 10 minutes. This process is carried out and repeated with the variation of the number of deposited layers: 2, 3, 4, and 5 layers. The coated substrates were subsequently dried to remove residual solvents and annealed at 500 °C for 1 hour to facilitate the crystallization of the tin oxide matrix and the incorporation of fluorine ions.

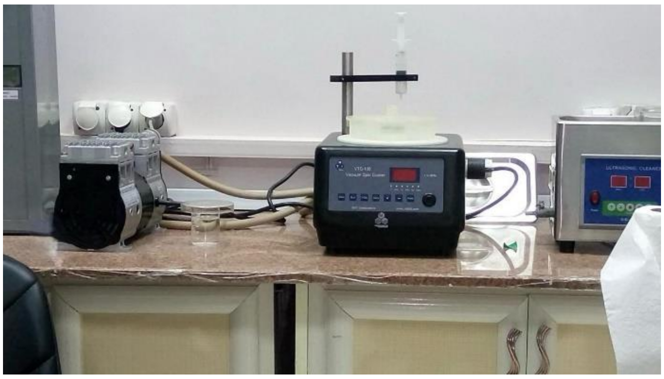

Fig. 2. Spin coating deposition mechanism

2.3 Characterization procedures

The crystalline structure of both pure and fluorine-doped SnO_2 thin films was examined using X-ray diffraction (XRD), performed on a Philips diffractometer equipped with Cu-Kα radiation ($\lambda=1.540\times10^{-10}$ m), operated at 40 kV and 30 mA. Scans were conducted in the Bragg-Brentano geometry. The diffraction patterns were used to assess phase purity, crystallinity, and structural changes induced by fluorine doping, including peak shifts and broadening indicative of lattice distortion and crystallite size variation. The surface morphology of thin films was analyzed using a scanning electron microscope (SEM, JEOL JSM-6360LA) to assess grain structure, uniformity, and surface texture. The SEM system was also equipped with an energy-dispersive X-ray spectroscopy (EDX) unit for elemental analysis. The spectral distribution of the optical transmission of the prepared samples has been recorded in the wavelength range of 300 to 900 nm using UV spectroscopy. The sheet resistance and the charge carrier concentration of fluorine-doped tin oxide thin films were determined using Hall effect measurements conducted at room temperature. A custom-built setup was employed, operating under an applied magnetic field of 0.96 T, see Fig. 3.

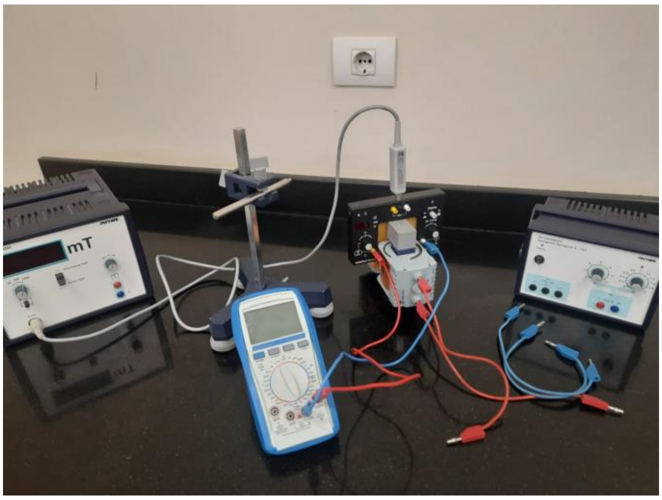

Fig. 3. Hall effect measurement setup

3 Results and discussion

3.1 Structural analysis

3.1.1 X-ray diffraction analysis

The X-ray diffraction (XRD) analysis was conducted on FTO thin films with fluorine concentrations of 10, 20, 30, and 40 wt%, deposited using both homemade spray pyrolysis and spin coating techniques, and annealed at 500 °C, as indicated in Figs. 4 and 5, respectively. All samples exhibited diffraction patterns consistent with the tetragonal rutile SnO_2 phase (JCPDS No. 41-1445), confirming the retention of the host crystal structure regardless of fluorine content or deposition method. Prominent peaks corresponding to the (110), (101), (200), (211), (310), and (301) planes were exhibited in all cases. As the fluorine concentration increased, a gradual shift of the diffraction peaks toward higher 2θ values was noted indicating a slight reduction in lattice parameters. This behavior is attributed to the substitution of smaller F^- ions for O^{2-} in the SnO_2 lattice.

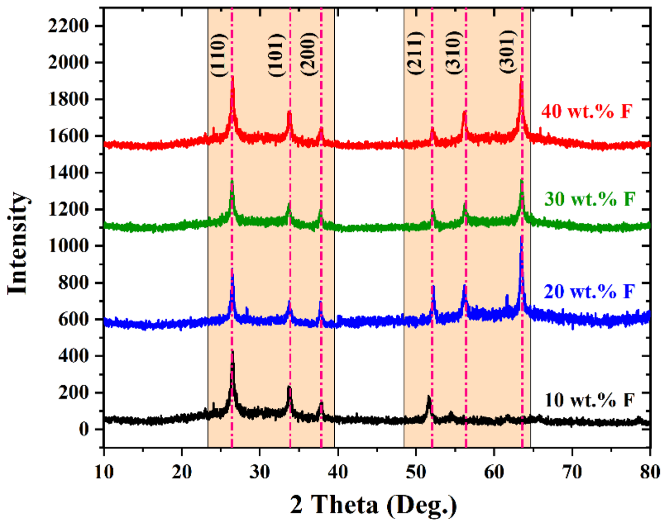

Fig. 4. XRD of FTO using the homemade spray technique

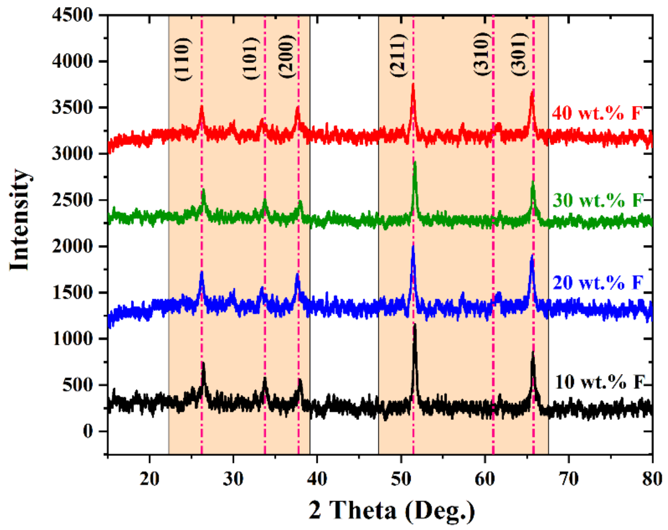

Fig. 5. XRD of FTO using the spin coating technique

Comparatively, films deposited by spray pyrolysis displayed sharper and more intense peaks, reflecting better crystallinity and larger crystallite sizes, whereas spin-coated films showed broader peaks, suggesting finer grains and possibly higher internal strain. The structural evolution with increasing fluorine content was more pronounced in the spin-coated films, where the incorporation of dopant appeared to more significantly affect the microstructure. Overall, both deposition techniques produced phase-pure FTO films, but the crystallinity and lattice behavior varied notably with dopant level and fabrication method.

Grain size D and dislocation density δ, key structural parameters, were estimated from the XRD patterns using Scherrer's formula given in the following equations [20]. The corresponding values are summarized in Tab. 1.

$$D = \frac{0.9\lambda}{\beta \cos\theta} \quad (1)$$

$$\delta = \frac{1}{D^2} \quad (2)$$

Here, λ denotes the X-ray wavelength 1.540×10^{-10} m, β represents the full width at half maximum (FWHM) of the diffraction peak, and θ is the corresponding Bragg angle. The calculated lattice parameters as a function of fluorine doping concentration are illustrated in Fig. 6. A noticeable trend is observed: as the concentration of fluorine increases, the crystallite size decreases. This inverse relationship suggests that higher doping levels introduce lattice disorder or strain, which impedes grain growth during crystallization. This behavior is likely due to the dopant atoms disrupting the long-range order, thus restricting grain boundary mobility and crystal coalescence.

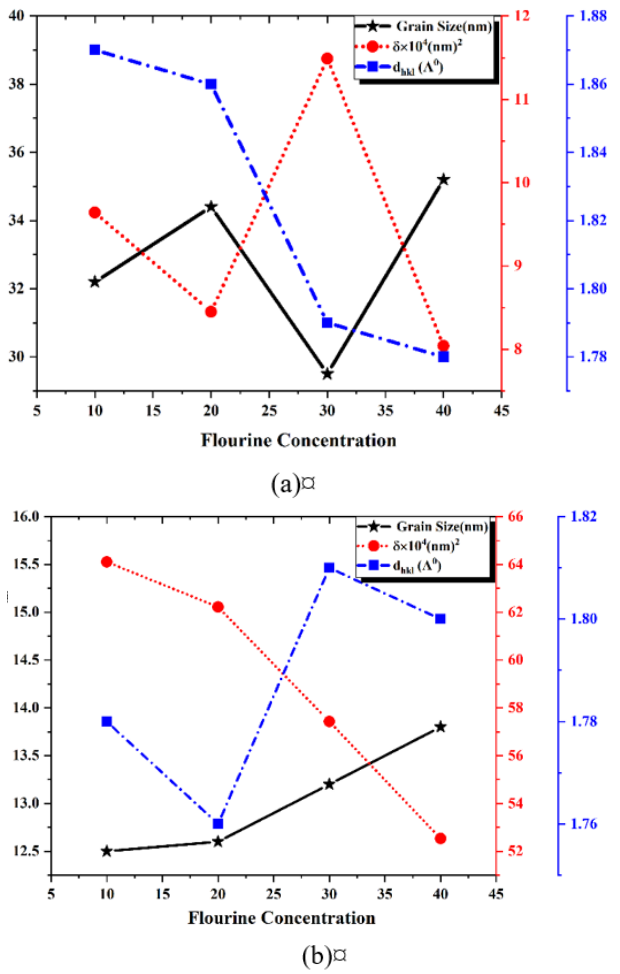

Fig. 6. Effect of fluorine doping on grain size, dislocation density, and interplanar spacing for FTO thin films deposited by (a) spray technique, and (b) spin coating

Additionally, an increase in both microstrain δ and dislocation density D is observed with increasing dopant concentration, as summarized in Tab. 1. These findings support the interpretation that dopant incorporation not only refines grain size but also induces structural defects within the crystal lattice, further affecting the film's microstructure.

Based on the XRD analysis, the lattice parameters a and c corresponding to the tetragonal phase were determined using established equations, as described in [21].

$$2d_{hkl}\sin(\theta) = n\lambda \tag{3}$$

$$\frac{1}{{d_{hkl}}^2} = \frac{h^2+k^2}{a^2} + \frac{l^2}{c^2} \tag{4}$$

In these calculations, d_{hkl} represents the interplanar distance, (*hkl*) are the Miller indices. The calculated values, presented in Tab. 1, show good agreement with standard reference data.

Table 1. Parameters of FTO thin films prepared with varying fluorine doping concentrations

Concentration (wt% of F)		d_{hkl} (10^{-10} m)	Lattice parameters		Grain size D (nm)	$\delta\times10^4$ (nm^{-2})	Texture coefficient
			a (10^{-10} m)	c (10^{-10} m)			
Spray deposition	10	1.87	4.71	3.21	32.2	9.64	0.78
	20	1.86	4.72	3.21	34.4	8.45	0.76
	30	1.79	4.72	3.22	29.5	11.49	0.83
	40	1.78	4.75	3.20	35.2	8.04	0.88
Spin deposition	10	1.78	4.75	3.24	12.5	64.11	0.68
	20	1.76	4.76	3.25	12.6	62.22	0.77
	30	1.81	4.75	3.25	13.2	57.43	0.87
	40	1.80	4.77	3.20	13.8	52.53	0.83

The intensity of the (*hkl*) diffraction peaks in the XRD pattern can be employed to evaluate the preferential orientation of crystallites within the thin film. Specifically, the relative intensity of each reflection provides insight into the degree to which grains are oriented in a particular crystallographic direction parallel to the sample surface. To quantify this, the texture coefficient (*TC*) for a given (*hkl*) plane can be calculated using the Harris texture analysis method defined by [22]

$$TC(hkl) = \frac{I(hkl)}{I_0(hkl)} \times \left[\frac{1}{n}\sum_{i=1}^{n}\frac{I(hkl)}{I_0(hkl)}\right]^{-1} \tag{5}$$

$I(hkl)$ is the measured intensity of the (*hkl*) reflection, $I_0(hkl)$ is the corresponding standard intensity from the JCPDS card, and n is the number of diffraction peaks considered. A $TC(hkl)$ value of 1 indicates random orientation, while values significantly greater than 1 imply a strong preferred orientation along that plane. This analysis enables identification of dominant growth directions in thin films, which is critical for tailoring the structural and functional properties of the deposited materials.

3.1.2 Surface morphology analysis

Optimizing the surface morphology and average grain size of conducting oxide films deposited on glass substrates plays a crucial role in optimizing the crystalline and optical performance of TCO films for advanced technological applications. The SEM was employed to investigate the prepared samples of FTO with different fluorine concentrations, as depicted in Figs. 7 and 8 for the two preparation methods of spray and spin coating deposition. The images reveal that the films possess a dense and uniform surface morphology, composed of compact, spherical-shaped crystalline grains in the nanoscale range

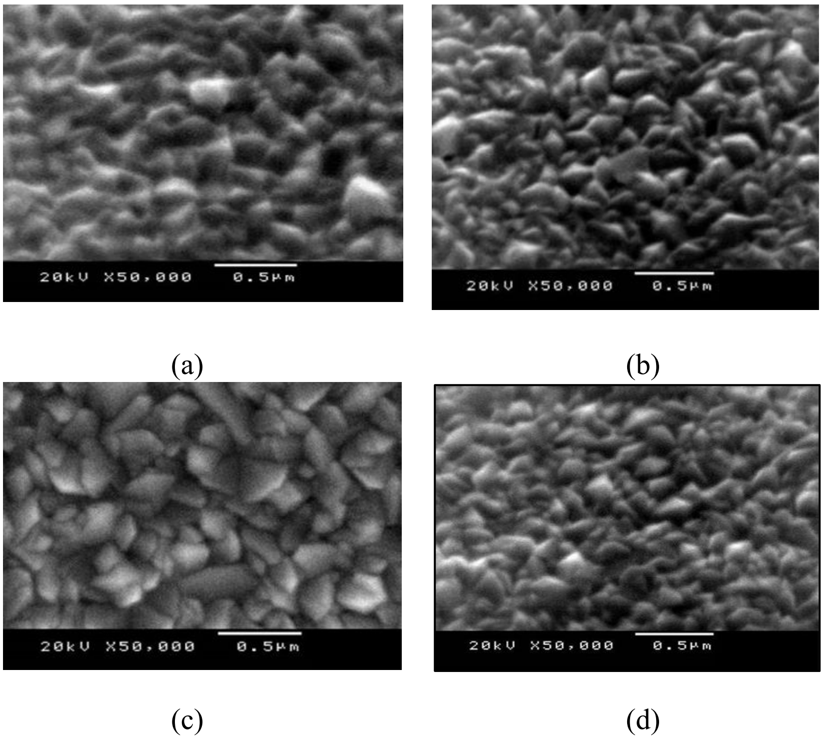

Fig. 7. SEM images of homemade spray deposition technique of FTO: (a) 10 wt% F, (b) 20 wt% F, (c) 30 wt% F, and (d) 40 wt% F

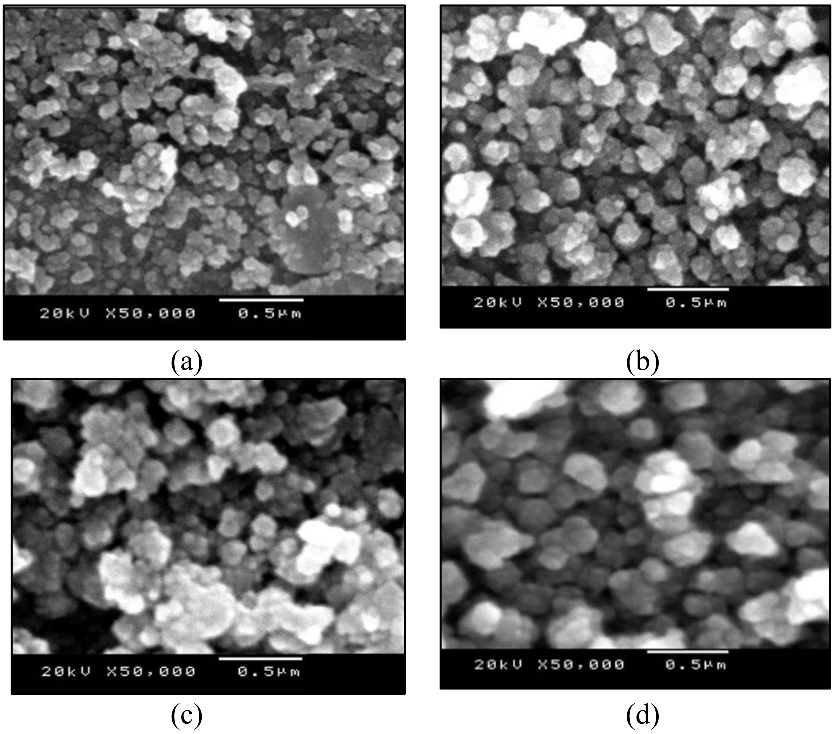

Fig. 8. SEM images of spin coating deposition technique of FTO: (a) 10 wt% F, (b) 20 wt% F, (c) 30 wt% F, and (d) 40 wt% F

EDX analysis revealed distinct peaks corresponding to Sn, O, and F elements, confirming the presence of these constituents in the FTO films. The results indicate that the elemental composition remains consistent with the expected FTO stoichiometry, as shown in Fig. 9.

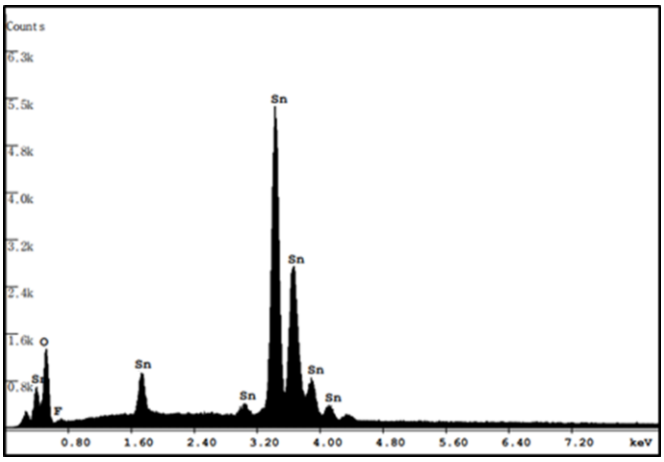

(a)

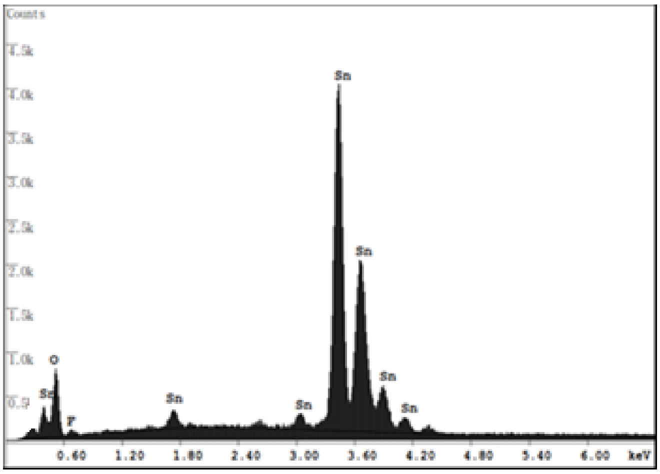

(b)

Fig. 9. EDX spectrum of the FTO thin films via (a) spray technique, and (b) spin coating

The grains of FTO exhibit good distribution and strong adhesion to the substrate, with no visible macroscopic defects such as voids or cracks. Furthermore, a noticeable reduction in average grain size is observed with an increasing fluorine doping level. The SEM figures of the prepared samples reveal distinct differrences in the microstructure of the films depending on both the fluorine concentration and the deposition method. FTO thin films deposited via spray pyrolysis exhibit smooth, dense morphology with spherical grains. As the fluorine concentration increases from 10 to 40 wt%, grain size decreases due to dopant-induced inhibition of atomic diffusion at grain boundaries. This results in limited grain growth and enhanced nucleation, promoting improved crystallinity and surface uniformity essential for optoelectronic applications. In contrast, spin-coated FTO films exhibit a more granular morphology with less uniform grain distribution and noticeable porosity at lower fluorine levels. Increasing fluorine concentration leads to smaller, more densely packed grains, though some surface inhomogeneity remains. These variations arise from the spin coating process's sensitivity to solution viscosity and film spreading dynamics during deposition.

Overall, both deposition methods confirm that increasing fluorine content refines the grain structure and enhances film compactness. Nevertheless, films produced via spray pyrolysis exhibit better crystallinity and surface homogeneity, likely due to more controlled thermal and deposition conditions.

3.2 Optical properties analysis

The optical properties of FTO thin films deposited by spray pyrolysis and spin coating were analyzed using UV-Vis spectroscopy in the 300-900 nm range. All films exhibited high optical transmittance (>80%) in the visible region. Spray-deposited films showed slightly higher average transmittance (~85%) compared to spin-coated films (~78%), attributed to their smoother surface and denser microstructure. A gradual blue shift in the absorption edge was observed with increasing fluorine content, and the calculated optical bandgap values increased from 3.61 eV (10 wt% F) to 3.82 eV (40 wt% of F), consistent with the Burstein–Moss effect. These findings underscore the significant impact of both deposition technique and fluorine doping concentration on the optical performance of FTO films, emphasizing their suitability for use in transparent electronic applications.

The film thickness t of the FTO samples was estimated from the interference fringes observed in the optical transmittance spectra, using the following relation described in [23].

$$t = \frac{\lambda_1 \lambda_2}{2[n(\lambda_1)\lambda_2 - n(\lambda_2)\lambda_1]} \quad (6)$$

In this expression, $n(\lambda_1)$ and $n(\lambda_2)$ represent the refractive indices at two adjacent maxima corresponding to the wavelengths λ_1 and λ_2. Furthermore, the refractive index n can be determined using the following equations:

$$n = \sqrt{N + \sqrt{(N^2 - n_s^2)}} \quad (7)$$

$$N = \frac{(n_s^2 + 1)}{2} + 2n_s \frac{T_{max} - T_{min}}{T_{max}.T_{min}} \quad (8)$$

In these equations, n_s represents the refractive index of the substrate, while T_{max} and T_{min} correspond to the maximum and minimum transmittance values at the same wavelength, as shown in the transmission spectra (Fig. 10). The influence of varying fluorine concentrations on the film thickness, as well as the electrical and optical properties of the FTO films, is summarized in Tab. 2. The optical absorption coefficient α can be derived from the measured transmittance T using the equation below [24].

$$T = e^{-\alpha t} \quad (9)$$

In this equation, t represents the thickness of the FTO and G-FTO films. The absorption coefficient α is subsequently used to estimate the optical band gap E_g through the Tauc relation [21]:

$$\alpha h\nu = C\left(h\nu - E_g\right)^{0.5} \quad (10)$$

The energy bandgap E_g is estimated by plotting $(\alpha h\nu)^2$ against $(h\nu)$, where α represents the absorption coefficient, h is Planck's constant, ν denotes the frequency of the incident photon, and C represents a constant for direct transitions. The bandgap is obtained by extrapolating the linear portion of the plot to the $(h\nu)$-axis at the point where $(\alpha h\nu)^2 = 0$. An increase in fluorine doping concentration in SnO_2 results in a noticeable widening of the band gap, consistent with trends reported in earlier studies. This bandgap widening is primarily attributed to the Burstein-Moss effect, wherein the increased carrier concentration fills the lower energy states of the conduction band, effectively shifting the absorption edge to higher photon energies [25]. Figure 11 illustrates the variation in energy bandgap of FTO thin films with different fluorine doping concentrations, emphasizing the significant impact of doping levels on the electronic properties of the material

3.3 Electrical properties analysis

The electrical characteristics of TCO thin films such as fluorine-doped tin oxide (FTO) are a fundamental indicator of their suitability for optoelectronic applications including solar cells, displays, and smart windows. In this study, detailed electrical characterization was performed using the Hall effect measurement technique as depicted in Fig. 3, which provides more comprehensive information than traditional methods such as the four-point probe. The Hall method enables direct quantification of key electrical parameters including sheet resistance R_{sh}, carrier concentration n, carrier mobility μ, and conductivity σ, offering deeper insight into the transport mechanisms within the material.

The Hall effect arises when a conducting sample carrying current I is subjected to a perpendicular magnetic field B. Due to the Lorentz force acting on the moving charge carriers, a transverse potential difference known as the Hall voltage V_H is developed across the sample. This voltage is used to determine the Hall coefficient R_H which is related to the type and concentration of the charge carriers:

$$R_H = \frac{V_H.t}{I.B} \quad (11)$$

Here, V_H denotes the Hall voltage, t represents the thickness of the film, I is the current through the sample, and B is the magnetic flux density. From R_H, the carrier concentration is calculated as:

$$n = \frac{1}{q.|R_H|} \quad (12)$$

Here, q represents the elementary charge. The electrical conductivity σ is given by the following formula

$$\sigma = q.n.\mu \quad (13)$$

The sheet resistance R_{sh}, which is critical for thin films, is calculated as

$$R_{sh} = \frac{1}{q.n.\mu.t} \quad (14)$$

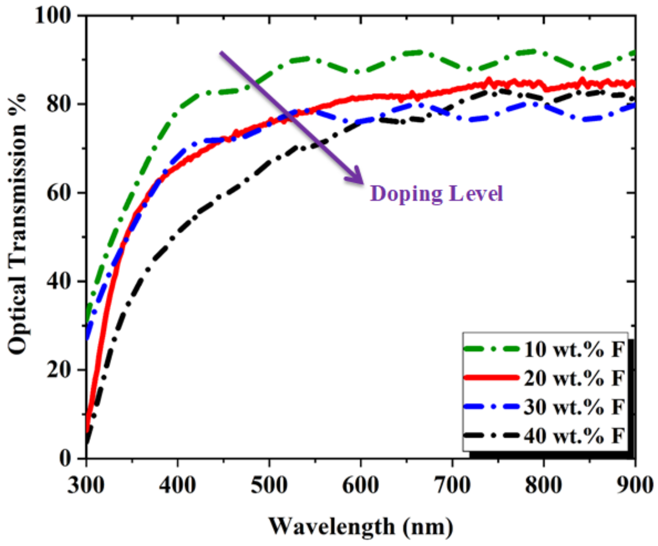

(a)

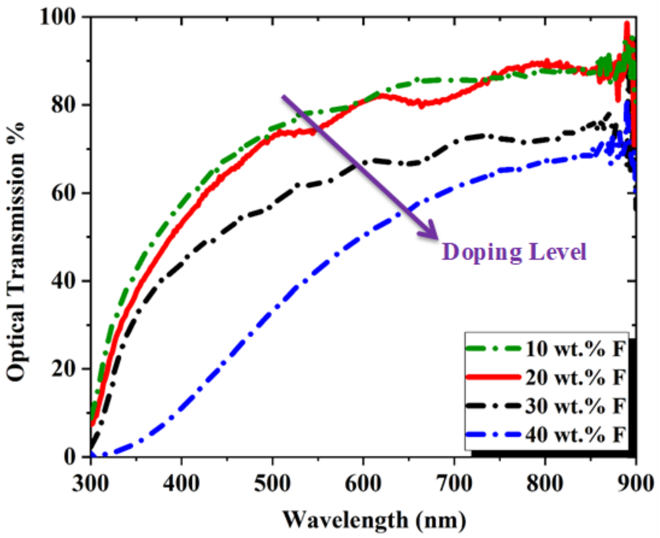

(b)

Fig. 10. Optical Transmission of FTO thin films: (a) spray technique, and (b) spin coating

This framework allows for a complete electrical profile of the thin films under investigation.

The electrical behavior of fluorine-doped tin oxide (FTO) thin films is largely governed by the doping concentration and resulting structural and electronic modifications within the SnO_2 lattice. In the pristine state, SnO_2 is an intrinsic n-type semiconductor with limited conductivity due to the scarcity of free carriers. Fluorine atoms F^-, when introduced via doping, replace oxygen atoms O^{2-} in the lattice due to their similar ionic radii and electronegativity. Each fluorine substitution contributes an extra free electron to the conduction band, thereby increasing the electron carrier concentration and enhancing the film's conductivity.

The figure of merit (FOM) serves as a crucial quantitative metric for assessing the overall performance of transparent conducting oxide (TCO) materials. It enables direct comparison between different TCO films by integrating both their electrical conductivity and optical transparency – two key parameters that determine their suitability for applications such as solar cells, displays, and optoelectronic devices. Over the years, researchers have proposed several formulations of the FOM to evaluate the effectiveness of TCOs under different functional requirements. Among these, the Haacke figure of merit $\emptyset_m$ is widely accepted for transparent electrodes, as it provides a balanced assessment of transparency and sheet resistance. It is expressed mathematically as:

$$\emptyset_m = \frac{T^{10}}{R_{sh}} \tag{15}$$

Here, T represents the average transmittance, and R_{sh} is the sheet resistance of the film (in Ω/□). A higher FOM indicates a more efficient TCO material, achieving low resistive loss while maintaining high optical transparency – essential for maximizing the performance of optoelectronic devices.

FTO thin films deposited by the spray pyrolysis technique exhibited strong electrical and optical performance, primarily due to the high substrate temperature (~500 °C) and the efficient thermal decomposition of precursor droplets during deposition. In this study, the fluorine doping concentration varied across 10, 20, 30, and 40 wt% of F to investigate its effect on the structural and functional properties of the films. Among the samples, the film with a thickness of 550 nm, corresponding to 30 wt% of F, demonstrated the most favorable performance – achieving a low sheet resistance of 20 Ω/□, optical transmittance of 80%, and the highest Haacke figure of merit (FOM) of 5.37×10^{-3} Ω^{-1}. These values indicate effective charge transport and transparency, attributed to enhanced crystallinity and film density at this fluorine concentration. As the fluorine content increased to 40 wt%, further growth in thickness (e.g., 750 nm and above) led to a decline in FOM, due to increased resistivity and reduced transmittance. On the other hand, lower fluorine levels (10-20 wt%) produced thinner films with higher transmittance (up to 88%) but also higher sheet resistance, limiting their electrical performance. These results confirm that spray pyrolysis, when combined with optimized fluorine doping – particularly at 30 wt% F – enables the fabrication of high-quality FTO films with an ideal balance between electrical conductivity and optical transparency. This makes them excellent candidates for use as transparent electrodes in photovoltaic applications.

FTO thin films prepared via the spin coating technique exhibited varying electrical performance depending on film thickness, with overall moderate conductivity compared to films prepared by spray pyrolysis. Spin coating remains a widely used, solution-based deposition method due to its simplicity, uniformity, and low-cost processing. However, the relatively low deposition temperature and reliance on post-annealing can adversely affect film densification and crystallinity. In this study, FTO thin films deposited via the spin coating technique exhibited a clear dependence of electrical and optical performance on film thickness. The thinnest film, at 420 nm, achieved the highest optical transmittance (82%), but also showed the highest sheet resistance (145 Ω/□) and a relatively low figure of merit (FOM) of $0.917\times10^{-3}\,\Omega^{-1}$, indicating poor electrical conductivity. As the thickness increased to 510 nm, electrical conductivity improved, with a reduced sheet resistance of 77 Ω/□, while transmittance remained high at 80%, resulting in a better FOM of $1.39\times10^{-3}\,\Omega^{-1}$. The most favorable performance was observed for the 840 nm thick film, which demonstrated a sheet resistance of 54 Ω/□, transmittance of 77%, and the highest FOM of $1.53\times10^{-3}\,\Omega^{-1}$, marking it as the most balanced in terms of transparency and conductivity. However, increasing the thickness further to 1050 nm led to a decline in transmittance to 72% and a modest increase in sheet resistance to 68 Ω/□, resulting in a drop in FOM to $0.813\times10^{-3}\,\Omega^{-1}$. These findings suggest that optimal performance in spin-coated FTO films is achieved at intermediate thicknesses, where a favorable balance between optical transparency and electrical conductivity is achieved. These results suggest that film thickness strongly influences optimizing the performance of spin-coated FTO, with intermediate thicknesses yielding the best balance of transparency and conductivity. The reduced mobility and higher resistivity in many of the spin-coated films are attributed to the presence of microstructural defects, smaller grain sizes, and void factors that increase carrier scattering and limit performance. Thus, while spin coating offers several processing advantages, further optimization of annealing conditions and doping levels is essential to enhance the structural and electrical quality of FTO films produced via this method.

The results of this study demonstrate that spray pyrolysis is the preferred deposition technique for fabricating FTO thin films with superior electrical and optical properties. Films prepared by spray pyrolysis exhibited higher optical transmittance and significantly lower sheet resistance compared to those produced by spin coating, as depicted in Tab. 2. This improvement is attributed to the formation of dense, uniform, and well-crystallized microstructures enabled by the high substrate temperature during the spray process. In contrast, spin-coated films showed higher resistivity and reduced transparency, largely due to structural imperfections such as smaller grains and increased porosity. While spin coating may be suitable for applications requiring low-temperature processing or flexible substrates, spray pyrolysis remains the more effective method for developing high-performance transparent electrodes where both high conductivity and excellent optical clarity are essential.

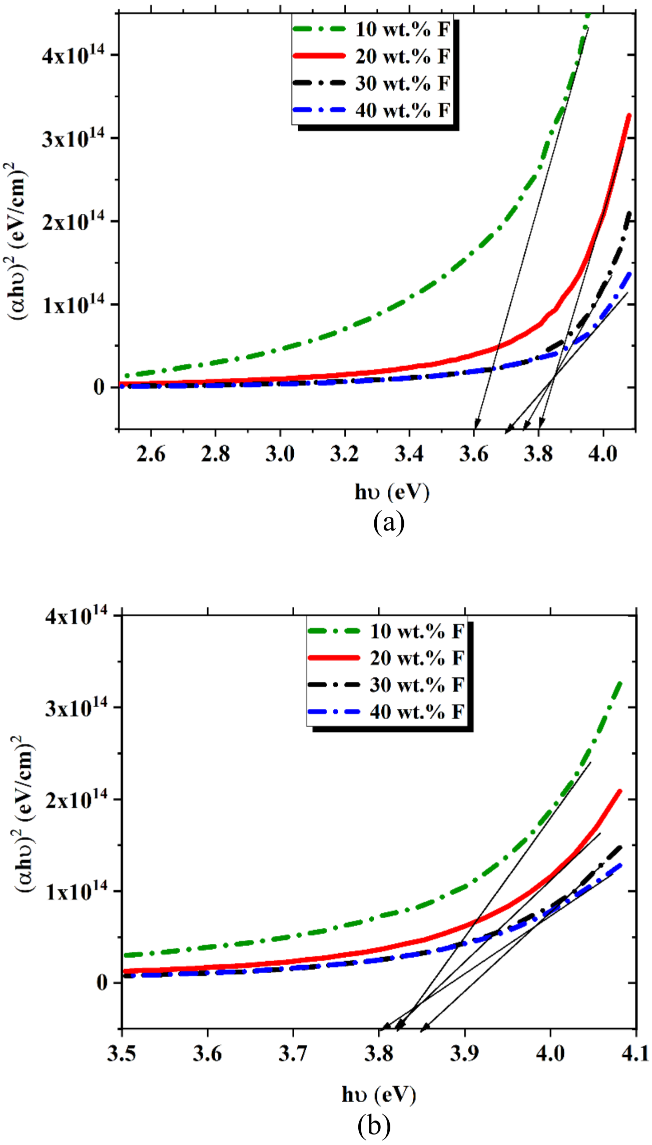

Fig. 11. Variation of optical energy band gap with fluorine doping concentration for FTO thin films synthesized using (a) spray pyrolysis, and (b) spin coating techniques

In this context, the employed preparation techniques and the optimized fluorine doping strategy confirm the effectiveness of the developed FTO thin films as promising candidates for advanced optoelectronic applications. To further highlight the performance of the fabricated samples, a comparative analysis is provided in Tab. 3, contrasting the electrical and optical characteristics of our spin-coated and spray-deposited FTO films with those reported in recent literature. The comparison reveals that our films, particularly those prepared via spray pyrolysis, exhibit superior FOM, low sheet resistance, and high transmittance – affirming the reliability and competitiveness of the proposed processing techniques for transparent conducting oxide applications.

Table 2. Effect of fluorine doping concentration on film thickness, optical transmittance, electrical conductivity, and energy bandgap of FTO thin films deposited via spray pyrolysisand spin coating techniques

Concentration (wt% of F)		Thickness (nm)	Transparency (%)	R_{sh} (Ω/□)	Resistivity ρ×10^{-3} (Ω.cm)	E_g (eV)	FOM $\emptyset_m$ (10^{-3} Ω^{-1})
Spray deposition	10	320	88	80	2.56	3.61	3.4
	20	380	85	55	2.09	3.82	3.58
	30	550	80	20	1.10	3.87	5.37
	40	750	77	30	2.25	3.67	2.76
Spin deposition	10	420	82	145	6.09	3.81	0.917
	20	510	80	77	3.93	3.8	1.39
	30	840	77	54	4.51	3.87	1.53
	40	1050	72	68	7.1	3.84	0.813

Table 3. Comparison of the results obtained in this study with recently published state-of-the-art reports on FTO thin films

Thickness (nm)	T (%)	R_{sh} (Ω/□)	E_g (eV)	Deposition temperature (°C)	$FOM\ \emptyset_m$ (10^{-3} Ω^{-1})	Deposition technique	Doping element	Reference
246	87	88	3.92	450	2.5	Spray	Sb	[26]
120	85	95	3.69	400	1.39	Spray	Sb	[27]
298	87.46	35.84	-	400	7.3	Spray	Sb	[28]
371	90.4	10.3	3.7	420	33	Spray	F	[29]
475	81.2	24	3.6	500	5.2	Spray	F	[30]
125	88.69	37.7	3.7	450	8.05	Nebulizer spray	F	[31]
780	82	15	3.8	500	9.16	Nebulizer spray	F	[8]
813	79	8	3.9	500	11.8	Nebulizer spray	F and Graphene	
-	65	-	3.2	300	-	Spin Coating	F	[32]
285	82	7	3.78	250	-	Spin coating	F	[33]
-	95	0.77	3.82	500	9.8	Spin coating	Undoped SnO_2	[34]
-	88	40	3.6	500	3.66	Spin coating	Ti	[35]
550	80	20	3.87	500	5.37	Spray	F	Proposed work
840	77	54	3.87	500	1.53	Spin Coating	F	

4 Conclusion

Fluorine-doped tin oxide (FTO) thin films were successfully synthesized via two low-cost deposition techniques – homemade spray pyrolysis and spin coating – at a substrate temperature of 500 °C with varying fluorine concentrations (10-40 wt%). Comparative analysis revealed that films fabricated by spray pyrolysis exhibited superior electrical and optical properties, achieving lower sheet resistance, higher transmittance, and enhanced figures of merit due to improved crystallinity and film uniformity. While spin-coated films demonstrated acceptable performance, their electrical quality was limited by increased defect density and grain boundary scattering. These results underscore the effectiveness of spray pyrolysis for producing high-quality FTO films and validate fluorine doping as a key strategy for optimizing transparent conductive oxides for optoelectronic applications.

References

[1] S. Hamdan, E. K. Hamad, H. A. Mohamed, and S. A. Khaleel, "High-performance MTM inspired two-port MIMO antenna structure for 5G/IoT applications," *Journal of Electrical Engineering*, vol. 75, no. 3, pp. 214–223, 2024.

[2] M. S. Abdel-Fattah, E. K. Hamad, T. G. Aboulnaga, S. A. Khaleel, and H. A. Elsadek, "Compact UWB microstrip patch antenna for 5G mobile handset applications," *International Journal of Microwave and Optical Technology*, vol. 18, no. 3, pp., 2023.

[3] N. Alsaab, K. Alhassoon, F. Alsaleem, F. N. Alsunaydih, S. O. Madbouly, S. A. Khaleel, and M. Shaban, "High-performance series-fed array multiple-input multiple-output antenna for millimeter-wave 5G networks," *Sensors*, vol. 25, no. 4, p. 1036, 2025.

[4] S. C. Ray, "Electrical, electronic and magnetic behaviours of F-doped SnO_2 thin film," *Bulletin of Materials Science*, vol. 45, no. 3, p. 142, 2022.

[5] R. A. Afre, N. Sharma, M. Sharon, and M. Sharon, "Transparent conducting oxide films for various applications: A review," *Reviews on Advanced Materials Science*, vol. 53, no. 1, pp. 79–89, 2018.

[6] V. Balaprakash, K. Thangavel, M. Mohan, P. Gowrisankar, and R. Sakthivel, "Thin film transparent conducting oxides and its anticorrosion and surface protection applications: A review," in *Novel Anti-Corrosion and Anti-Fouling Coatings and Thin Films*, pp. 109–127, 2024.

[7] J. Patel, R. K. Sharme, M. A. Quijada, and M. M. Rana, "A review of transparent conducting films (TCFs): Prospective ITO and AZO deposition methods and applications," *Nanomaterials*, vol. 14, no. 24, p. 2013, 2024.

[8] S. A. Khaleel, M. Shaban, M. F. Alsharekh, E. K. Hamad, and M. I. Shehata, "Preparation and characterization of graphene-based fluorine doped tin dioxide thin films via spray pyrolysis technique," *Journal of Electrical Engineering*, vol. 74, no. 6, pp. 463–473, 2023.

[9] M. Rahayi, M. H. Ehsani, A. C. Nkele, M. M. Shahidi, and F. I. Ezema, "Synthesis and characterization of tin (IV) oxide thin films," *Optical and Quantum Electronics*, vol. 53, no. 5, p. 222, 2021.

[10] J. T. Wang, X. L. Shi, W. W. Liu, X. H. Zhong, J. N. Wang, L. Pyrah, and K. Tsuri, "Influence of preferred orientation on the electrical conductivity of fluorine-doped tin oxide films," *Scientific Reports*, vol. 4, no. 1, p. 3679, 2014.

[11] M. Hinna, B. Hartiti, A. Gouya, H. Labrim, S. Fadili, M. Tahri, and P. Thévenin, "Synthesis of ITO thin films by spray pyrolysis based on Taguchi design," *Materials Today: Proceedings*, vol. 66, pp. 447–455, 2022.

[12] R. S. R. K. U. Rathnayakage, T. M. W. J. Bandara, K. Wijayaratne, G. R. A. Kumara, L. A. de Silva, and K. Tennakone, "Fluorine-doped tin oxide thin films with high surface conductance and low transparency for boosting performance in dye-sensitized solar cell applications," *ACS Applied Energy Materials*, vol. 6, no. 16, pp. 8336–8348, 2023.

[13] A. Nath, J. A. Salam, A. M. Anand, A. Raj, and R. Jayakrishnan, "Solar cells using spray coated a-axis grown F: SnO_2 thin films," *Optical Materials*, vol. 159, p. 116612, 2025.

[14] J. Zhou, X. Tian, R. Chen, W. Chen, X. Meng, X. Guan, and W. Chen, "An ultra-thin chemical vapor deposited polymer interlayer to achieve highly improved stability of perovskite solar cell," *Chemical Engineering Journal*, vol. 461, p. 141914, 2023.

[15] H. Latif, J. Liu, D. Mo, R. Wang, J. Zeng, P. F. Zhai, and A. Sattar, "Effect of target morphology on morphological, optical and electrical properties of FTO thin film deposited by pulsed laser deposition for $MAPbBr_3$ perovskite solar cell," *Surfaces and Interfaces*, vol. 24, p. 101117, 2021.

[16] I. Y. Bu, "Sol–gel deposition of fluorine-doped tin oxide glasses for dye sensitized solar cells," *Ceramics International*, vol. 40, no. 1, pp. 417–422, 2014.

[17] B. L. Zhu, H. Peng, Y. Tao, J. Wu, and X. W. Shi, "Highly transparent conductive F-doped SnO_2 films prepared on polymer substrate by radio frequency reactive magnetron sputtering," *Thin Solid Films*, vol. 756, p. 139360, 2022.

[18] M. B. Saleh, M. B. Soliman, S. A. Khaleel, and M. Adel, "Structural, morphological, optical and electrical properties of SnO_2: F thin films via nebulizer spray and electro-spinning techniques," *Journal of Advanced Research in Materials Science*, vol. 41, pp. 19–26, 2018.

[19] T. Arini, L. H. Lalasari, N. C. Natasha, F. E. Yunita, F. Firdiyono, A. Syaputra, … and A. Subhan, "Controller of fluorine-doped tin oxide thin films deposition via cycles and annealing temperatures by spin coating techniques," *Vostochno-Evropeyskiy Zhurnal Peredovykh Tekhnologiy*, vol. 5, no. 12-107, pp. 57–65, 2020.

[20] R. J. Deokate, S. M. Pawar, A. V. Moholkar, V. S. Sawant, C. A. Pawar, C. H. Bhosale, and K. Y. Rajpure, "Spray deposition of highly transparent fluorine doped cadmium oxide thin films," *Applied Surface Science*, vol. 254, no. 7, pp. 2187–2195, 2008.

[21] A. Rahal, A. Benhaoua, M. Jlassi, and B. Benhaoua, "Structural, optical and electrical properties studies of ultrasonically deposited tin oxide (SnO_2) thin films with different substrate temperatures,"*Super lattices and Microstructures*, vol. 86, pp. 403–411, 2015.

[22] C. S. Man, "Determination of texture coefficients via X-ray diffraction," in *Crystallographic Texture and Group Representations*, Dordrecht, Netherlands: Springer, 2023, pp. 223–247.

[23] A. S. Ibraheam, J. M. Rzaij, M. A. Fakhri, and A. W. Abdulwahhab, "Structural, optical and electrical investigations of Al: ZnO nanostructures as UV photodetector synthesized by spray pyrolysis technique," *Materials Research Express*, vol. 6, no. 5, p. 055916, 2019.

[24] Z. Y. Banyamin, P. J. Kelly, G. West, and J. Boardman, “Electrical and optical properties of fluorine doped tin oxide thin films prepared by magnetron sputtering,” *Coatings*, vol. 4, no. 4, pp. 732–746, 2014.
[25] A. Benhaoua, A. Rahal, B. Benhaoua, and M. Jlassi, “Effect of fluorine doping on the structural, optical and electrical properties of SnO_2 thin films prepared by spray ultrasonic,” *Superlattices and Microstructures*, vol. 70, pp. 61–69, 2014.
[26] K. Derrar, M. Zaabat, N. Rouabah, R. Nazir, F. Hanini, A. Hafdallah, and K. M. Abualnaja, “Preparation of Sb: SnO_2 thin films and its effect on opto-electrical properties,” *Journal of Materials Science: Materials in Electronics*, vol. 33, no. 13, pp. 10142–10153, 2022.
[27] M. F. Hossain, M. A. H. Shah, M. A. Islam, and M. S. Hossain, “Transparent conducting SnO_2 thin films synthesized by nebulized spray pyrolysis technique: Impact of Sb doping on the different physical properties,” *Materials Science in Semiconductor Processing*, vol. 121, p. 105346, 2021.
[28] S. Gürakar and T. Serin, “High quality optoelectronic properties of Sb-doped SnO_2 by spray pyrolysis with less solution,” *Materials Research Express*, vol. 6, no. 8, p. 086423, 2019.
[29] K. H. Kim, B. R. Koo, and H. J. Ahn, “Sheet resistance dependence of fluorine-doped tin oxide films for high-performance electrochromic devices,” *Ceramics International*, vol. 44, no. 8, pp. 9408–9413, 2018.
[30] E. Ching-Prado, A. Watson, and H. Miranda, “Optical and electrical properties of fluorine doped tin oxide thin film,” *Journal of Materials Science: Materials in Electronics*, vol. 29, no. 18, pp. 15299–15306, 2018.
[31] R. Ramírez-Amador, G. Flores-Carrasco, S. Alcántara-Iniesta, J. Rodríguez González, O. García-Teniza, E. Mercado-Agular, and A. B. Vásquez-Ortiz, “Structural, morphological, optical, and electrical characterization of fluorine doped tin oxide (FTO) thin films synthesized by PSP,” *Solid State Phenomena*, vol. 286, pp. 64–71, 2019.
[32] E. Yustanti *et al.*, "Fabrication of fluorine-doped tin oxide by using Indonesian local stannic chloride precursors with spin coating method," in *IOP Conference Series: Materials Science and Engineering*, 2020, vol. 909, no. 1, p. 012092: IOP Publishing.
[33] M. N. A. Bitu, N. I. Tanvir, S. Islam, and S. F. U. Farhad, “Effect of substrate surface on the wide bandgap SnO_2 thin films grown by spin coating,” *MRS Advances*, vol. 8, no. 5, pp. 194–200, 2023.
[34] H. Meddas, L. Abdelghani, D. Amel, B. Saliha, S. Randa, and B. Okba, “Spin coating deposition of tin oxide thin films: Influence of solution concentration,” *Journal of Chemical Research*, vol. 48, no. 5, p. 17475198241277728, 2024.
[35] P. Sivakumar, H. S. Akkera, T. R. K. Reddy, Y. Bitla, V. Ganesh, P. M. Kumar, … and M. Poloju, “Effect of Ti doping on structural, optical and electrical properties of SnO_2 transparent conducting thin films deposited by sol-gel spin coating,” *Optical Materials*, vol. 113, p. 110845, 2021.

Sherif A. Khaleel received his B.E. and M.Sc. degrees in Electronics and Communication Engineering from the Arab Academy for Science, Technology and Maritime Transport (AASTMT), Egypt, in 2012 and 2017, respectively. He obtained his Ph.D. in Electrical Engineering from Aswan University in 2023, where his research focused on the design of graphene-based microstrip patch antennas in the THz band for future 6G communication systems. Dr. Khaleel is currently an Assistant Professor in the Department of Electronics and Communication Engineering at the College of Engineering and Technology, AASTMT, Aswan, Egypt. His research interests include antenna design, metamaterials, THz and mm-wave technologies for 5G/6G communications, reconfigurable intelligent surfaces (RIS), and microwave imaging for breast cancer detection. He serves as a reviewer for several reputable journals, including IEEE Access, Scientific Reports, Radioengineering, Progress in Electromagnetics Research (PIER), The Journal of Electrical Engi-neering, Plasmonic, Alexandira Engineering Journal, Ain Shams Engineering Journal and Optical and Quantum Electronics.

Ahmed M. Abdelsamad received his B.Sc. degree in Electronics and Communication Engineering from the Arab Academy for Science, Technology and Maritime Transport (AASTMT) in 2019. He is currently serving as a Teaching and Research Assistant in the Department of Basic and Applied Sciences at the College of Engineering and Technology, AASTMT. He is actively involved in teaching undergraduate courses and supporting laboratory work, while also contributing to research in the areas of renewable energy and control systems. His research interests include solar cell technologies, optimization methods, digital control techniques, and power system stability.

Gaber Magdy was born in Qena, Egypt, in 1989. He received the B.Sc. and M.Sc. (Hons.) degrees in electrical engineering from Aswan University, Egypt, in 2011 and 2014, respectively, and the jointly supervised Ph.D. degree in electrical engineering from Kyushu Institute of Technology in Japan, and Minia University in Egypt, in 2019. He began his journey at Aswan University, Egypt, by joining the Electrical Engineering Department, Faculty of Energy Engineering, Aswan University, as a Demonstrator in December 2011, an Assistant Lecturer in November 2014, an Assistant Professor in September 2019, and an Associate Professor in September 2024. From 2017 to 2019, he was a Visiting Researcher Fellow with the Department of Electrical and Electronic Engineering at Kyushu Institute of Technology, Japan. In 2022, he was a Postdoctoral Fellow with the Department of Electrical Engineering, University of Jaén, Spain. Additionally, in 2024, he was a Postdoctoral Fellow with the Bardely Department of Electrical and Computer Engineering, Virginia Tech., Blacksburge-Virginia, U.S. Currently, he is an Associate Professor (fully seconded) at the Faculty of Engineering, King Salman International University, South Sinai, El Tor, Egypt. His research interests include power system stability, dynamics, and control, smart/micro-grid control, renewable energy, energy storage systems, and digital control techniques, all applied to power systems. He has authored or coauthored two international books, and over 80 peer-reviewed papers on stability, dynamics, and control of renewable power systems in reputed international journals and conferences.

Mohamed I. Shehata obtained his B.E. and M.Sc. degrees in Electronics and Communication Engineering from the Arab Academy for Science, Technology and Maritime Transport (AASTMT), Egypt, in 2004 and 2009, respectively. He later earned his Ph.D. in Electrical Engineering from Aswan University, Egypt, in 2017. He currently holds the position of Head of the Electronics and Communication Engineering Department at the College of Engineering and Technology, AASTMT, Aswan Campus. Alongside his teaching duties, Dr. Shehata is actively involved in supervising both undergraduate and postgraduate research projects and contributes to various academic development initiatives. His research interests span a broad range of topics, including optical engineering, optical fiber communication systems, nonlinear fiber optics, erbium-doped fiber amplifiers (EDFAs), optical amplifiers, microwave-optical communication, Li-Fi systems for indoor and outdoor applications, and optical sensing technologies aimed at next-generation mobile networks. He also serves as a peer reviewer for several international scientific journals in the areas of photonics, optical communications, and wireless technologies.

Nehad A. Zidan received the B.Sc. degree in Civil Engineering from Helwan University, Faulty of Engineering-Mataria, Cairo, Egypt in 2001 and M.Sc. degree in Engineering Physics from Mansoura University, Cairo, Egypt, in 2008 on the application of Laser on Thin Films. He obtained Ph.D. degree in Engineering Physics from Ain Shams University, Cairo, Egypt in 2013 on the effect of Magnetic Field on Fluid. He is an Associate Professor at the Department of Engineering Physics and Mathematics Department, Faculty of Engineering – Mataria, Helwan University, Cairo, Egypt. His research interests include solar cell technologies, optics, nano-fluids materials, and the areas of renewable energy.

Received 1 August 2025